Deep-Sea Research, Vol 39 No 11/12, pp 2029–2051, 1992
Printed in Great Britain

0198-0149/92 $5.00 + 0.00
Pergamon Press Ltd

A study of the Iceland–Faeroe Front using GEOSAT altimetry and current-following drifters

PAVEL PISTEK* and DONALD R. JOHNSON*

(*Received* 26 *February* 1991, *in revised form* 30 *December* 1991, *accepted* 27 *January* 1992)

Abstract—In this study we investigate the utility of GEOSAT altimetry for monitoring the Iceland–Faeroe frontal zone. Since an expected dynamic topography relief of 10–20 cm over the Iceland–Faeroe Front (IFF) was not much above the 10 cm uncertainty in GEOSAT observations, validation by AVHRR imagery and satellite-tracked drifters constituted an important part of the experiment. Sea Surface Height (SSH) relief of greater than 20 cm occurred along the western side of the IFF and along the eastern side, north of the Shetland Islands. However, with SSH relief of only 10–15 cm in the central region of the IFF, substantial difficulties were encountered in the ability to unambiguously monitor the location of the front. In contrast, frontal meanders with 20–30 cm SSH relief, current speeds up to 50 cm s^{-1} and radii of curvature of 25 km, were clearly observed on three occasions during the 2 year study. These meanders first appeared north of the Faeroe Islands, in the region from 6 to 8°W, and propagated southeastward at speeds of about 3.3 km day^{-1}, being lost from view in the Faeroe–Shetland Channel. Their strong signals and lifetimes of 2–3 months would appear to make them important constituents of IFF dynamics.

1. INTRODUCTION

THE Iceland–Faeroe frontal zone marks the oceanographic boundary between warm waters of the North Atlantic and relatively cool waters of the Greenland–Iceland–Norwegian (GIN) Seas. It is a dynamic area resulting from the confluence of basin-scale circulation patterns, and characterized by the frequent passages of intense atmospheric storms. Local bathymetry, especially the Iceland–Faeroe Ridge, strongly affects the circulation and distribution of water masses, and plays an important climatic role as a soft barrier between the North Atlantic and GIN Sea basins.

Interest in this area has spawned a long history of scientific study. HELLAND-HANSEN and NANSEN (1909) gave an early, and classic, description of circulation and water masses. TRANGELED (1973, 1974) provided historical summaries of measurements to about 1973, and HOPKINS (1988) further summarized the literature and the physical description for the period 1972–1985. JOHANNESSEN (1986) gave an additional summary of the physical oceanography of the Nordic Seas, including the Iceland–Faeroe region, and SMART (1984) provided an overview of the fronts in our region of interest.

Using these overviews, together with our present analysis, a rough schematic of currents

*Naval Oceanographic and Atmospheric Research Laboratories, Remote Sensing Branch, Stennis Space Center, MS 39529, U.S.A.

and fronts in the Iceland–Faeroe region can be developed (Fig. 1). Although the area is complex, and highly variable, two thermal fronts (fronts are defined here as boundaries between water masses with differing surface temperatures) have been known to systematically occur around Iceland and the Faeroe Islands. A relatively weak front begins in the Denmark Straits and passes around the north of Iceland, fading as it approaches the Iceland–Faeroe Ridge. This front (the Kolbeinsey Front) marks the separation of relatively warm Atlantic Waters of the Irminger/North Icelandic Currents, from cool waters of both the East Greenland Current (in the Denmark Straits) and the southern limb of the Norwegian Sea circulation (north and east of Iceland). This front is most clearly defined in surface expressions of thermal contrast during winter and least clearly defined during summer (SMART, 1984).

A second front, with somewhat stronger surface thermal contrast, begins along the eastern Icelandic continental shelf, and extends eastward along the northern flank of the Iceland–Faeroe Ridge. This Iceland–Faeroe Front (IFF) is formed when cool, highly modified North Atlantic Water (Irminger Current), flowing around the north side of Iceland (North Icelandic Current or Kolbeinsey Current), re-encounters warm North Atlantic Waters over the Ridge

Large distortions in the IFF have been observed near the Icelandic side of the ridge (10–12°W), where southward penetration of cool waters over the Iceland shelf, and adjacent northward penetration by Atlantic Waters form a large loop in the frontal position around 64 5°N, 11°W. HANSEN and MEINCKE (1979) have published locations of the front over a 5 year period from 1952 to 1957 showing the loop as a distinctive, but highly variable, feature.

Intersecting the Iceland–Faeroe Ridge near the 500 m depth contour on its northern flank, the IFF is tilted (progrades) upward toward the north, with lighter North Atlantic Waters on the south side riding up onto the Icelandic Current Waters on the northern side. In cross-section, the water mass interface is well defined by relatively strong, but density compensating, horizontal gradients in temperature and salinity. The density contrast between the two water masses at this point is only about 0.2 σ-$_t$ units, a fairly weak dynamic signature. Current meter data, collected in 1975/1976 (DOREY, 1978), indicated a characteristic eastward flow of approximately 20 cm s^{-1} in the upper layer (to 250 m) for moorings placed along the north face of the Ridge. Using the geostrophic relationship, this roughly corresponds to a sea surface height differential of about 13 cm across a 50 km wide front. ROBINSON *et al.* (1989) suggest that characteristics of the front include a maximum current speed of 25–50 cm s^{-1}, frontal width of 25–75 km and expected altimetric signals of 10–35 cm.

The surface manifestation of the IFF is highly variable in space and time. Hydrographic surveys from HANSEN and MEINCKE (1979) and GOTTHARD (1974) and, more recently, Airborne eXpendable BathyThermograph (AXBT) surveys by SMART (1984), BOYD *et al.* (1987) and BOYD (1988) clearly demonstrate this variability. Repeated surface mappings indicate that strong lateral excursions in the front occur with periodicities on the order of days. This rapid motion also has been observed in measured currents which, according to WILLEBRAND and MEINCKE (1980), have time scales over the Ridge of about 10 days and result from frontal baroclinic instabilities. In addition, the area over the Ridge, but south of the IFF, is characterized by numerous cyclonic and anticyclonic eddies These eddies, with scales of 30–40 km, are observed near the frontal zone, sometimes advected into place and sometimes formed in association with the large lateral excursions, or meanders It is

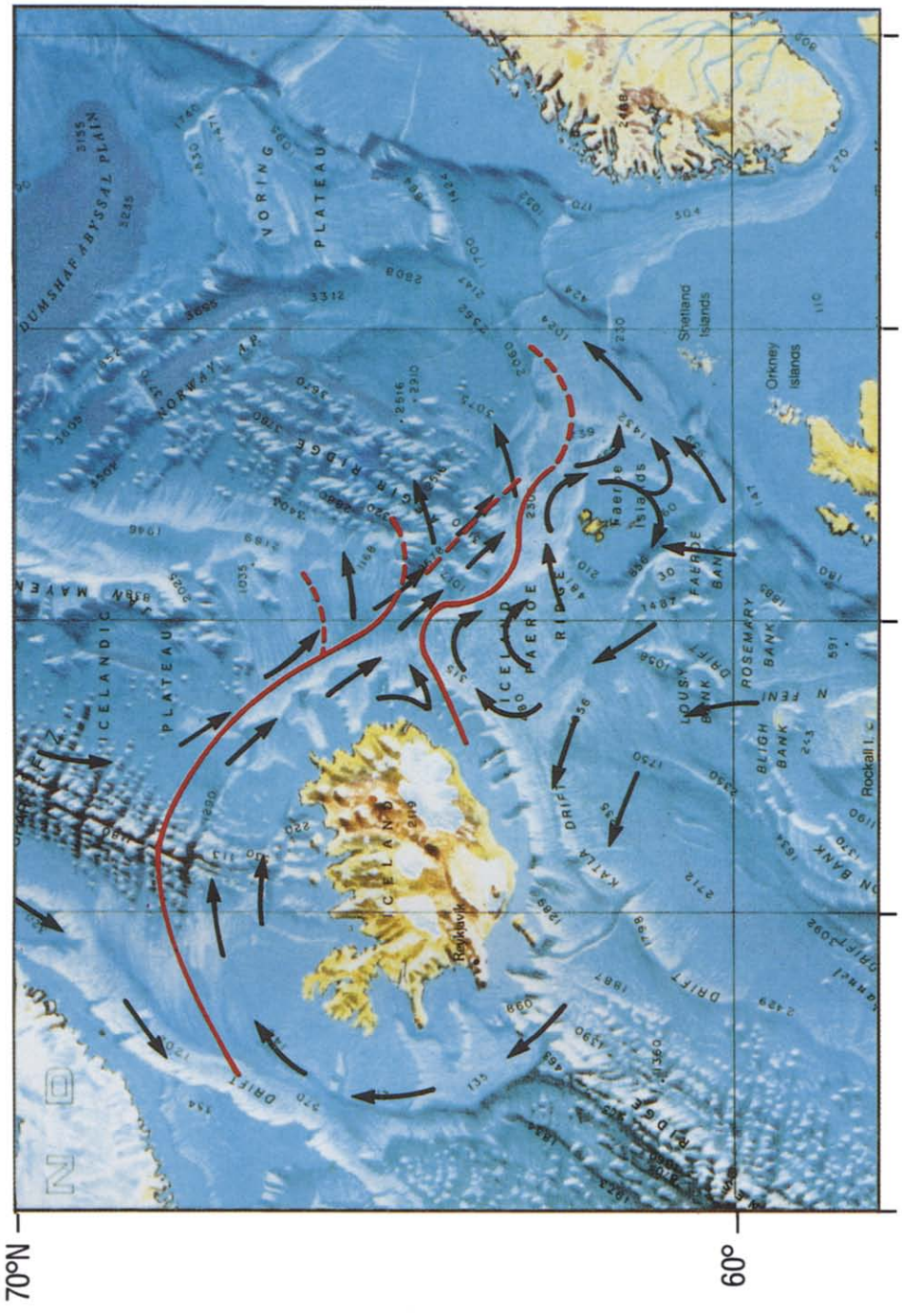

Fig. 1 Schematic drawing of currents (black arrows) and fronts (red lines) overlaying bottom topography (*World ocean floor*, by Bruce C. Heezan and Marie Tharp, 1977. © 1977 Marie Tharp)

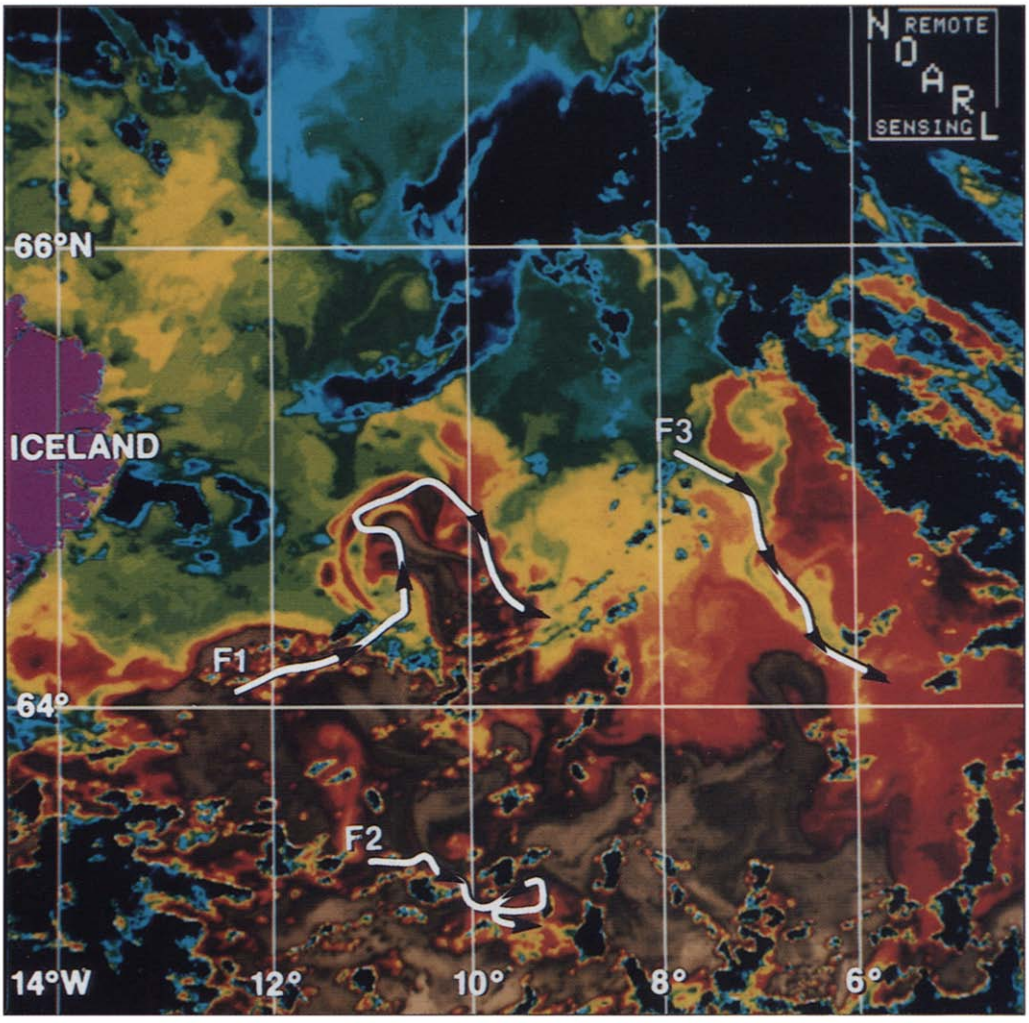

Fig. 7 False color composited image from NOAA-9 AVHRR passes on 8 and 9 November 1988 Tracks of drifters F1, F2 and F3 cover 2 weeks surrounding the image dates The Iceland–Faeroe Front is located between brown and red, the Kolbeinsey front is located between dark green and light green Note the weakening of the thermal gradient across the IFF east of 8 5°W

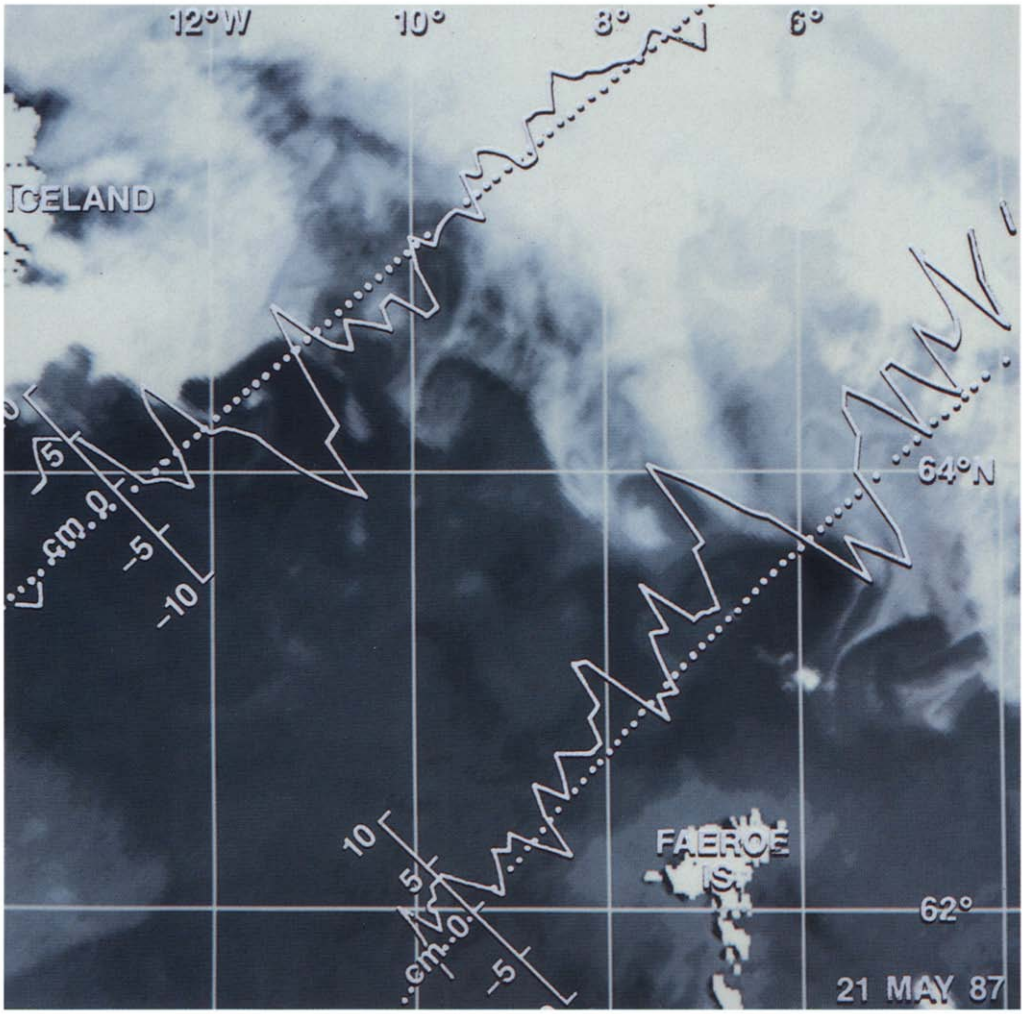

Fig 12 NOAA-9 AVHRR image on 21 May 1987, with SSH profiles from descending tracks D21 (upper) and D16 (lower) Track D21 shows a cyclonic eddy on the IFF (Fig 11), and track D16 shows an anticyclonic meander on the IFF

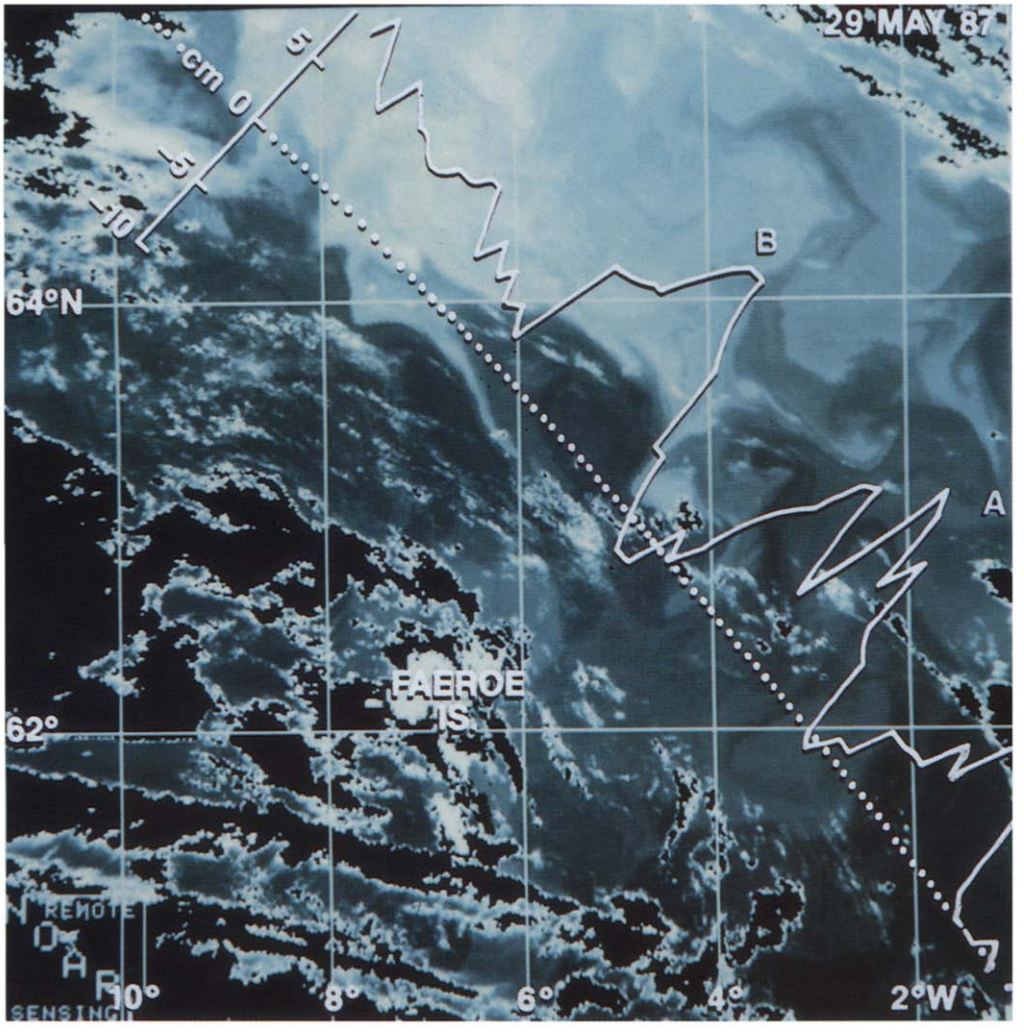

Fig 13 NOAA-9 AVHRR image on 29 May 1987, showing meanders "A" and "B" The SSH profile is from ascending track A12 on 2 June 1987 (Fig 14)

reasonable to expect that these vigorous circulation features will enhance mixing across the frontal boundary (Scott and McDowall, 1990)

Monitoring the Iceland–Faeroe region, with its rapid time scales, small space scales and relatively weak dynamic signatures, has posed a considerable problem. Because of thermal contrasts across the front, Infra-Red (IR) imagery from satellites has been useful at times. However, frequent cloudiness makes passive imagery both difficult and unreliable. In contrast, the satellite-borne altimeter provides measurements in most weather conditions After proper corrections for a variety of geophysical error sources, the altimeter has shown success in other, stronger signature regions, in its ability to monitor front and eddy locations (e.g Cheney and Marsh, 1981; Lybanon *et al.*, 1990; Mitchell *et al* , 1990).

This study is focused on interpretation of altimetric signals from the U.S. Navy's GEOSAT (GEOdetic SATellite) satellite in the Iceland–Faeroe region. This is an area of expected surface height signatures of approximately 10–20 cm, which is just slightly larger than expected uncertainties from orbital and geophysical errors. Although correlations of altimeter signals with oceanographic measurements in the Norwegian Sea proper have been encouraging (e.g. Johannessen, 1984; Pistek *et al.*, submitted) there has been difficulty in interpreting altimetric residuals within the Iceland–Faeroe frontal zone (e.g. Robinson *et al* , 1989; Dobson, 1988). One of the principal reasons for the difficulties appears to be due to major errors in tidal corrections (Tomas and Woodworth, 1990). In this study, we have used an improved tidal model for tidal corrections.

The purpose of this study is to investigate the Iceland–Faeroe frontal zone using a combination of satellite data (GEOSAT altimetry and AVHRR imagery) and current-following surface drifters We correlate *in-situ* observations with features found from satellite sensors in an attempt to produce a better understanding of the IFF as well as an understanding of the capability of satellite-borne altimeters to monitor this relatively weak signal region

2 DATA COLLECTION AND TREATMENT

2.1 *Altimeter*

Figure 2 shows selected GEOSAT tracks across the Iceland–Faeroe area where altimeter data were collected during the Exact Repeat Mission (ERM) (see Born *et al* , 1987). This altimetric mission started on 8 November 1986, and continued until the satellite finally failed in January 1990. During the ERM, the ground track pattern repeated every 244 revolutions (17.05 days) with a resulting crosstrack spacing of about 45 km in the GIN Sea.

Primary altimeter data processing at the Naval Oceanographic and Atmospheric Research Laboratory (NOARL) consisted of data quality checks, removal of satellite orbital height, alongtrack averaging (to obtain one sample per second—about 7 km alongtrack spacing) and corrections for tides and electromagnetic (EM) bias. In order to compare tidal corrections, tides were computed with both the Schwiderski model (Schwiderski, 1980) and the Proudman Oceanographic Laboratory model (Flather, 1981). Further details of the primary processing procedures can be found in Lybanon *et al.* (1990). Secondary processing consisted principally of defining a "reference" ocean surface, from averages of sea-level on each track, and extracting sea surface height (SSH)

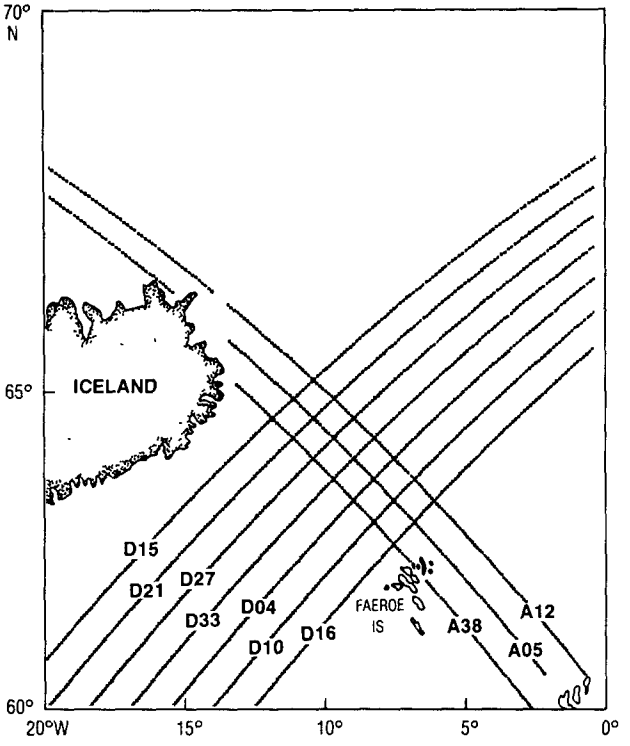

Fig 2 Ground tracks of GEOSAT altimeter during the ERM Track numbers beginning with a "D" represent descending tracks, and those beginning with an "A" represent ascending tracks

variations about this surface. Finally, the application of linear detrending to SSH residuals reduced the long wavelength orbit error (e.g. TAI, 1989; MITCHELL *et al.*, 1990)

Altimetric data were processed for a 2 year period, from April 1987 to April 1989. Numerous data dropouts occurred due to off-nadir mispointing of the altimeter. Thirty-eight per cent of the descending passes and 47% of the ascending passes were deemed useable in our region of interest. Dropouts of data occurred more frequently as the altimeter aged. This posed a considerable problem since positive identification of oceanographic features requires either ancillary data or repeatable identification.

Precision of the GEOSAT range measurement is estimated by MACARTHUR *et al* (1987) as 3.5 cm. Orbits were determined by the Navy Astronautical Group with a radial position uncertainty of 3 m. Since the predominate radial error occurs at the frequency of once per revolution, simple detrending, as discussed above, was considered to be adequate to reduce the residual orbit error to centimeter level (MITCHELL *et al.*, 1990). This linear fit also removes other geophysical errors (with wavelengths >1000 km) present in altimeter data. A detailed error budget for the GEOSAT mission and the list of assumptions upon which this budget is based are given in LYBANON and CROUT (1987). Over distance scales of 100 km or less, the uncertainty in topographic relief, from all sources, is estimated to be around 10 cm for the GEOSAT altimeter.

Commonly used for tidal corrections, the Schwiderski tide model is a global model with 1 degree resolution in latitude and longitude This resolution has proven to be adequate

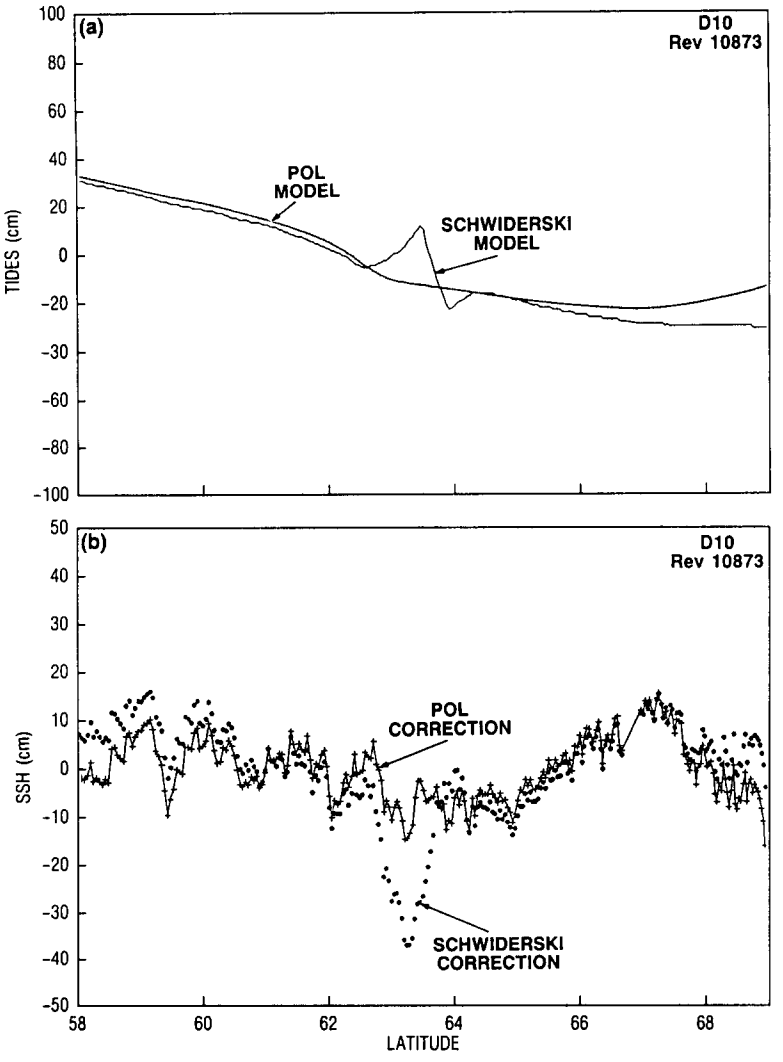

Fig 3 (a) Comparison of tide corrections along GEOSAT track D10 from the Schwiderski model and the POL model (b) Corrections from the two models applied to SSH from GEOSAT Note that the Iceland–Faeroe Front lies between 62°N and 64°N, where the large "kink" in the Schwiderski modeled tide gives a false indication of frontal location

over the deep ocean where tidal spatial scales are large. Over the Iceland–Faeroe Ridge area, however, tides are extremely complex, with relatively short spatial scales. Referring to Fig. 3, the large "kink" in tidal elevation from the Schwiderski model is located over the Ridge where the IFF is expected to occur, and produces a false signal of about 22 cm amplitude. This is at least as large as the expected real ocean dynamic topography, and occurs with similar spatial scales. In contrast, a tidal model with 1/3 degree latitude by 1/2 degree longitude grid, developed at the Proudman Oceanographic Laboratory (FLATHER, 1981; VASSEY, personal communication) provides a much smoother, and more realistic correction (see also THOMAS and WOODWORTH, 1990). After correction with the POL tidal

model, energy with wavelengths of several hundreds of kilometers can still be observed in the altimeter data (e.g. see Fig. 11, later). Although this is thought to be remaining unresolved tidal errors, the wavelengths are sufficiently long for satisfactory separation from frontal scales.

2.2. *Current drifter data*

To measure the surface current and, hence, to establish an estimate of expected dynamic topography relief, six ARGOS-tracked drifters were deployed for this experiment in the area of the Iceland–Faeroe frontal zone. These current-following drifters were designed at NOARL with small freeboard, and drogued with a canvas cross at 15 m depth Intermediate buoyancy disconnected the drogue from surface wave motion. With 9.5 m^2 frontal area, the drogue provided a 1/40 ratio between air and wetted areas, insuring minimal direct wind influence.

Five of the drifters lasted for an average of nearly 3 months, covering the area of interest quite well (Table 1). One of these five drifters lost its drogue after 47 days. Drifter locations were interpolated to common daily intervals, and velocities were computed from these daily positions. Absolute accuracy of the drifters' positions is given by the ARGOS system as ± 100 m. At a current speed of 10 cm s^{-1}, averaged over 1 day, this gives an estimated error in calculated dynamic topographic relief, from this one source, of about 0.1 cm over 50 km.

Wind stress data for the period were obtained from the Fleet Numerical Oceanographic Center's wind analysis. Using air pressure, thermal winds were computed at 2 5° latitude and longitude intervals, and brought to the 10 m level with a boundary layer model. Wind stress was calculated for the 10 m height using a drag coefficient of 2×10^{-6} cgs

3 RESULTS

3.1. *Drifters*

A composite of all drifter tracks is presented in Fig. 4. Drifters F1, F2 and F3 were deployed in mid-October, 1988; drifters F4, F5 and F6 were deployed in early to mid-November, 1988 (Table 1). Since F6 lasted only 6 days, it will not be further discussed. All five drifters spent at least part of their lifetime in southeastward motion along a northwest/southeast line running from the deployment location of F4 to the Faeroe–Shetland Channel. F1 and F2 converge on this "line" by basically eastward drift, although their

Table 1 *Drifter deployment schedule*

Drifter	Date deployed	Lat (°N)	Long (°W)	No days
F1	14 Oct 88	63 79	12 48	115
F2	14 Oct 88	64 31	11 11	103
F3	16 Oct 88	65 33	8 82	42
F4	6 Nov 88	67 60	14 27	111
F5	15 Nov 88	66 10	9 55	77
F6	16 Nov 88	64 53	10 74	4

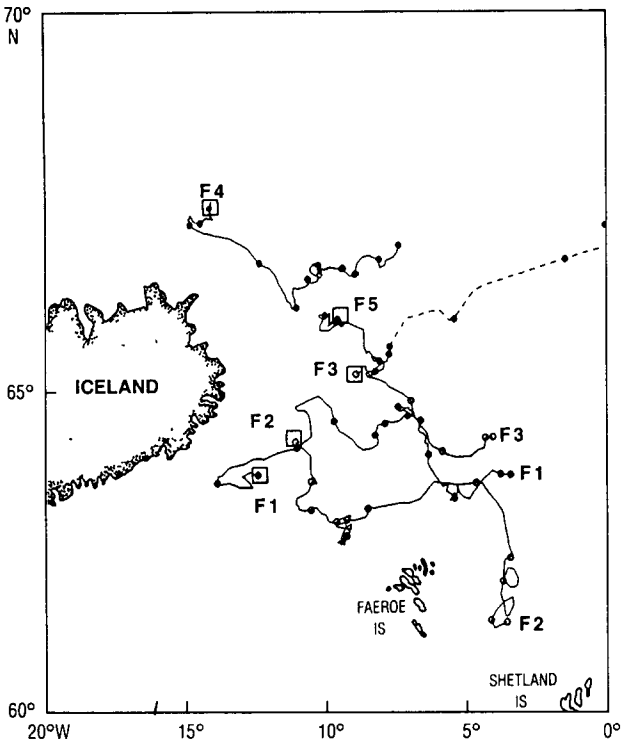

Fig 4 Tracks of five drogued drifters Table 1 gives the deployment schedule The square symbols represent launch locations, dots along the tracks are locations at 10 day intervals The dotted line represents the track of F5 after it lost its drogue

intermediate motions are highly convolved. Several of the drifters peel off the line at different times with motion into the interior of the Norwegian Sea, and one of the drifters (F2) moves southward, off the end of the line and into the Faeroe–Shetland Channel.

Before interpreting these motions in terms of the oceanographic information, it is necessary to demonstrate that the drifters are principally governed by currents and not by direct action of the winds Mean wind stress during this period follows the climatological pattern of flow around the atmospheric Icelandic Low (Fig. 5), with mean wind blowing across the Ridge from the Atlantic into the Norwegian Sea. Wind stress variability is much higher than its mean, as expected, since this is an area dominated by frequent passages of intense storms (Fig. 5). Orientation of the variability is relatively weak, with the principal axis of variation more or less perpendicular to the Ridge.

In order to correlate wind stress and drifter current vectors, the wind stress was interpolated from its sample pattern (Fig. 5) to the temporal position of each drifter. Although strong variability can be seen in space as well as time in wind stress and drifter current vectors (Fig 6), visual comparison of these sets indicates very little relationship between specific large wind events and current events. This weak relationship can be verified by a vector correlation of the wind series and current series.

Drifters F1, F2 and F3 showed no significant correlation with wind stress (Table 2). Drifters F4 and F5—the most northern of the drifters—showed statistically significant

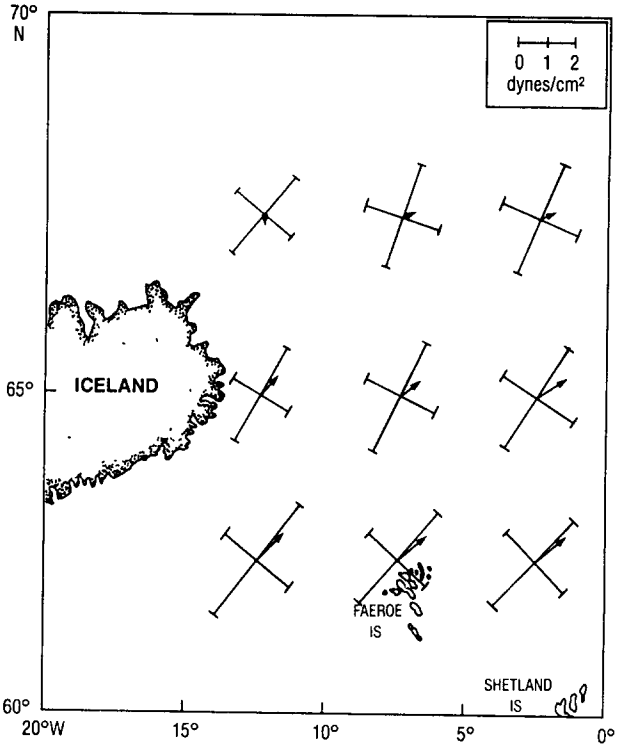

Fig 5 Vector means and principal axis of variation of wind stress during the time of deployment of the drifters Wind stress was calculated from FNOC wind analysis

correlation at an R-level of 0.29 and 0.40, respectively. This means, however, that only 9–16% (R^2) of the variation in F4 and F5 is related to the winds. Both F4 and F5 were correlated at about 60° to the right of the wind stress, about what could be expected for turning in an Ekman spiral, considering the 15 m depth of the drogues. Direct wind action on the drifters would tend to cause a downwind motion (as implied in the angle correlation of F5 after it broke free of its drogue). From the correlation analysis, then, it seems reasonable to conclude that direct wind action on the drifters was not important for our study. The wind influence that did occur, occurred north of the IFF proper and was probably related to flow characteristics in a wind driven surface layer, not to direct action of the winds on the surface buoy.

Drifters F3, F4 and F5 appear to follow the Kolbeinsey Front from north of Iceland to its final dissipation north of the Faeroe Islands (very weak thermal contrast can be seen in AVHRR images—i.e Fig. 7). Calculated current speeds in this flow are characteristically 6–8 cm s^{-1}. Assuming geostrophic balance and a frontal scale of 50 km, these speeds would be related to surface dynamic topography relief of about 5 cm across the Kolbeinsey Front, much too low to be detected from the GEOSAT altimeter.

Although contaminated by clouds, drifter tracks superimposed on an AVHRR image composited from two passes of NOAA-11 on 8 and 9 November 1988 (Fig. 7) indicates excellent agreement between thermal imagery and drifter motion. The track of F1 can be readily observed following the surface thermal manifestation of the IFF on its western

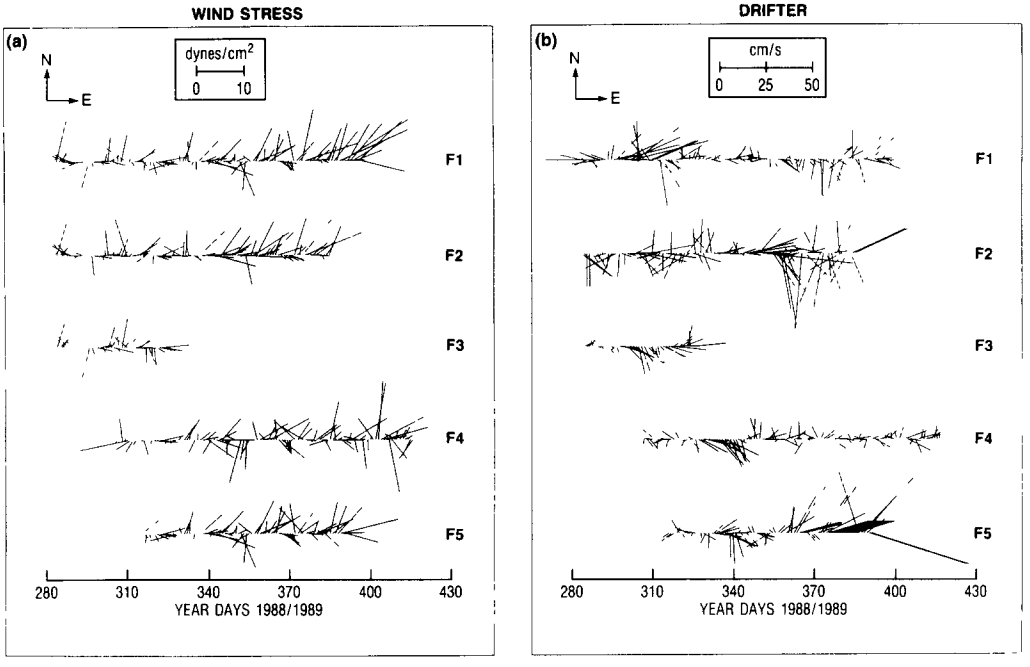

Fig 6 (a) Wind stress vector time series, from FNOC wind analysis, interpolated to the instantaneous location of each drifter (b) Current vector time series, from daily sampled location of each drifter

edge along the East Iceland shelf, and delineating the northward "loop" at about 64 5°N, 10.5°W. The highly convoluted nature of the IFF is apparent in Fig. 7. Drifter F3 followed the Kolbeinsey Front toward its dissipation and convergence with the IFF. Drifter F2 appears to have been caught in a cool, cyclonic eddy south of the IFF, and is drifting eastward. The remaining drifters are under clouds at this time.

In addition to being highly convoluted, the IFF also appears to vary considerably in strength (Fig. 8). Although F1 appears to have followed the IFF for nearly 3 months, the flow speed varies considerably: from 30–40 cm s^{-1} on the western side, to less than 10 cm s^{-1} in the center, and increasing to 15–25 cm s^{-1} on its eastern side. From the IR

Table 2 Vector correlation—wind stress/drifter velocity

Drifter	No pts	*R*	Phi†	Significant
F1	115	0 04	47 3	No
F2	103	0 08	58 9	No
F3	42	0 10	−18 4	No
F4	111	0 29	61 4	Yes
F5*	77 (47)	0 40 (0 40)	16 4 (59 2)	Yes

*Drifter F5 broke free of its drogue The two values given above are for the entire period and for the period up to its release (parenthesis)

†Positive correlation angle (phi) means that the drifter vector is to the right of the wind stress, negative to the left

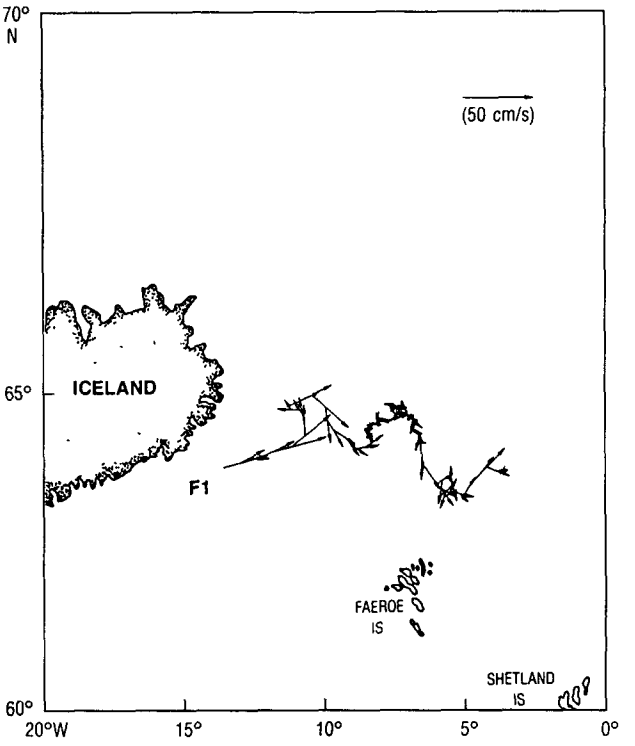

Fig 8 Daily drift vectors from drifter F1 along the IFF showing relatively large changes in speed

image in Fig 7, the thermal gradient appears to considerably weaken east of about 8.5°W. We can expect, then, that dynamic topography relief across the front also will vary, although it is not evident from the drifters if the variations are spatial, temporal, or both.

Since the drifters appear to have served well in following current patterns, they can be used to calculate expected surface dynamic topography relief through the assumption of local geostrophic balance. Figure 9 shows positions where SSH relief of greater than 10 and 20 cm, over a distance of 50 km, were calculated from daily average drifter speeds. Although the spatial/temporal distribution of the drifters is not capable of giving a complete picture of expected SSH topography, some interesting patterns begin to emerge. SSH relief, over 50 km, of greater than 10 cm is prevalent throughout the area. However, relief of greater than 20 cm is seen only on the western side of the IFF (along the East Iceland shelf) and on the eastern side (north and east of the Faeroe Islands). Throughout the central part of the IFF, relief of less than 20 cm means that we should anticipate difficulties in separating altimeter feature identifications out of the expected uncertainty level (10 cm).

3.2. *Altimeter*

As previously discussed, we have defined a reference surface by taking averages along an altimeter track. Although this method does eliminate the dominating geoid signal, it also creates several problems, including distortion of the signal and concomitant reduction

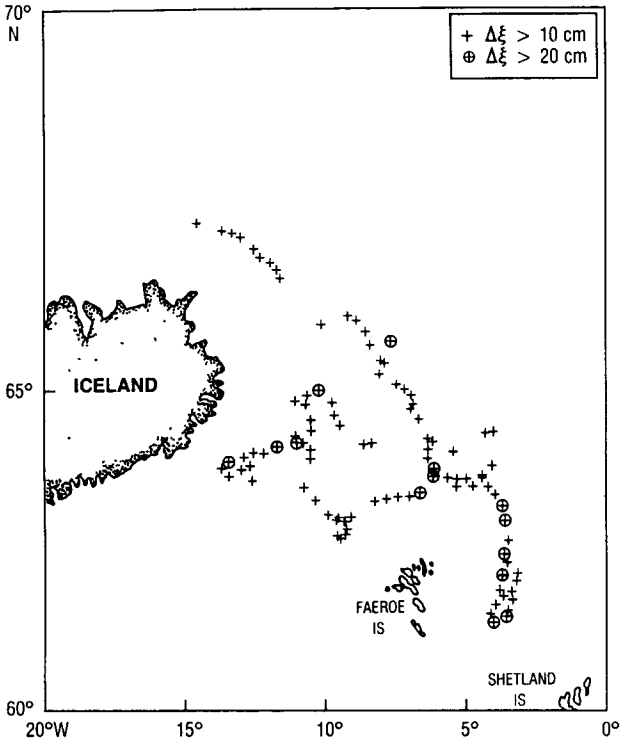

Fig 9 Using an assumption of geostrophic balance, calculations were made of expected SSH slope from drifter speeds The plus symbols represent locations where estimated SSH relief of greater than 10 cm over 50 km occurred, and the circle symbols represent SSH relief of greater than 20 cm over 50 km

of the signal amplitude (e.g. PORTER, 1988). Rather than look for a SSH slope commenserate with the IFF (i.e. sloping upward toward the south), we are forced to look for slope variations, regardless of direction.

The RMS variability of the altimeter-derived alongtrack SSH slope was formed by simply taking the difference between SSHs at 50 km separation, for each point on the track, and determining the RMS variability for all passes along that track. When presented in this fashion (Fig. 10), the most striking feature is an area of weak variability which tends to outline the northern edge of the IFF. South of this edge, and in the Faeroe–Shetland Channel, variability appears to be strong. This tends to confirm our notion that the Ridge is an area active with mesoscale eddies and frontal meanders, and that the IFF tends to inhibit northward migration of this energy.

SSH residuals from sequential descending passes along single tracks were examined for indications of presence of the IFF (e.g. Fig. 11). No feature appeared which could be defined unambiguously as the IFF or the Kolbeinsey Front without reference to ancillary data. The features which do appear have amplitudes of about 10–15 cm in relief. Although the drifter data was taken at a different time, this does confirm the surface relief estimate from drifter speeds in the central area of the IFF. Outside of the region where the IFF or Kolbeinsey Front could be expected, e.g. along 61–62 and 68°N, repeatable features (at 17

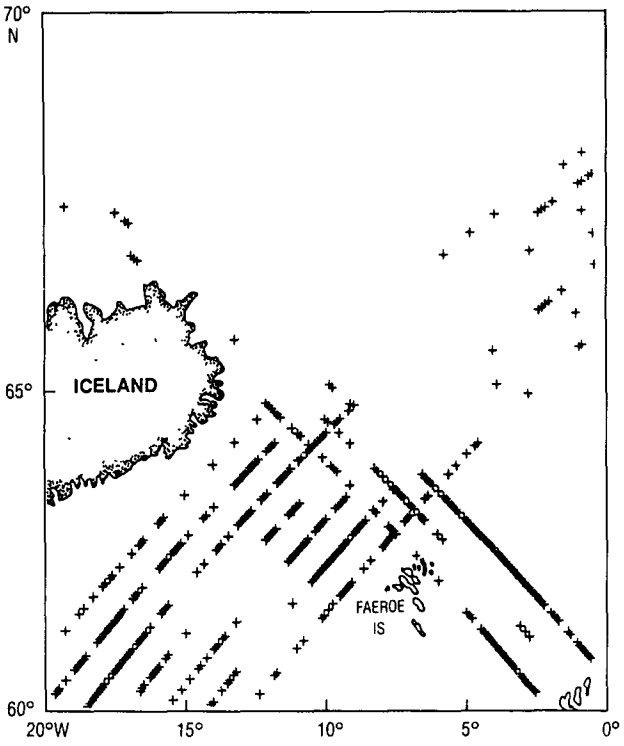

Fig 10 Locations where the RMS variability of GEOSAT-determined alongtrack SSH slope exceeded 7 5 cm/50 km We consider this variability to be an estimate of mesoscale activity Note the area of weak variability to the north of the IFF

day intervals) appear, with amplitudes of 15–25 cm in relief (Fig. 11). It seems reasonable to assume that the altimeter is, at least, capable of resolving this level of SSH relief.

The marked feature (Fig 11) at about 64°N in the mid-May and early June 1987 tracks, is a cyclonic eddy on the IFF. This is confirmed in a concomitant AVHRR image, presented with an altimeter track overlay (Fig. 12). It should be noted that, although this eddy has a relief of 10–15 cm and defines the IFF with its north wall, it would be difficult to identify unambiguously in the altimeter SSH profiles without the aid of AVHRR. Several cyclonic eddies are visible both on and south of the IFF (Fig. 12).

A second feature (Fig. 12), directly north of the Faeroe Islands with surface relief of 15–20 cm, can be seen in both the AVHRR image (21 May 1987) and in a SSH profile along track D16. This feature is an anticyclonic meander of the IFF with a radius of curvature of about 25 km. Eight days later, the meander (identified as meander "B") can be seen in a subsequent AVHRR image (Fig. 13—29 May 1987), with an eastward displacement of about 25 km clearly observable between the two images. Fortunately, the ascending altimeter track, A12, passed almost directly along the IFF, and captured this meander in its SSH profile (2 June 1987—also shown in Fig. 13).

To examine further these interesting, and relatively strong meander features, a sequence of eight consecutive ascending SSH profiles along track A12 is presented in Fig. 14. These passes, at 17 day intervals, show a southeastward movement of the meander at

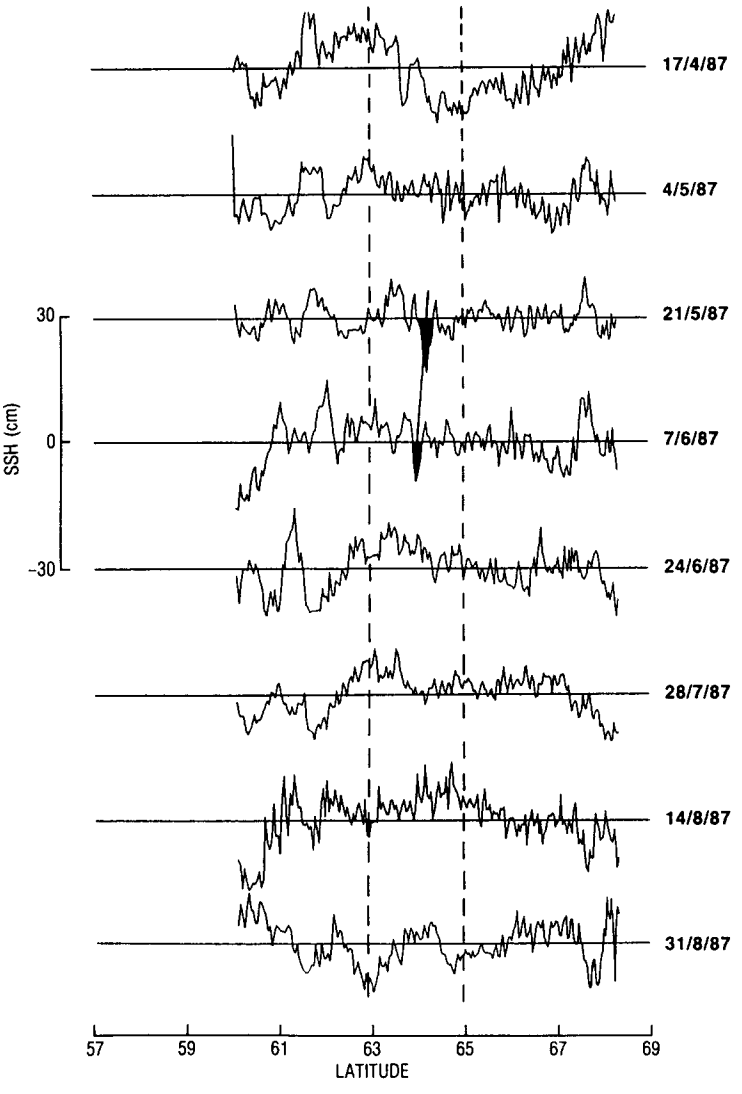

Fig 11 Sequential SSH residuals at 17 day intervals along descending track D21 (Fig 2) The vertical dotted lines represent latitudinal boundaries for the expected location of the IFF, the Kolbeinsey Front should occur at about 65°N Note repeating features, of 15–25 cm relief, outside of the marked boundaries The marked feature on 21 May and 7 June is identified as a cyclonic eddy on the IFF (Fig 12)

about 3.8 cm s^{-1} (3.3 km day^{-1}). A previous meander, identified as meander "A", is also discernible. Meander "A" propagates southeastward and terminates, or is lost from view, in the Faeroe–Shetland Channel. This latter meander also is seen in the western side of the Channel (Fig. 13). Although its IR signature is very weak in that location, its SSH amplitude remains relatively high.

A sequence of six ascending (A12) SSH profiles from 1988 (Fig. 15), also shows a strong meander feature on the IFF (defined as meander "C") Amplitudes and eastward

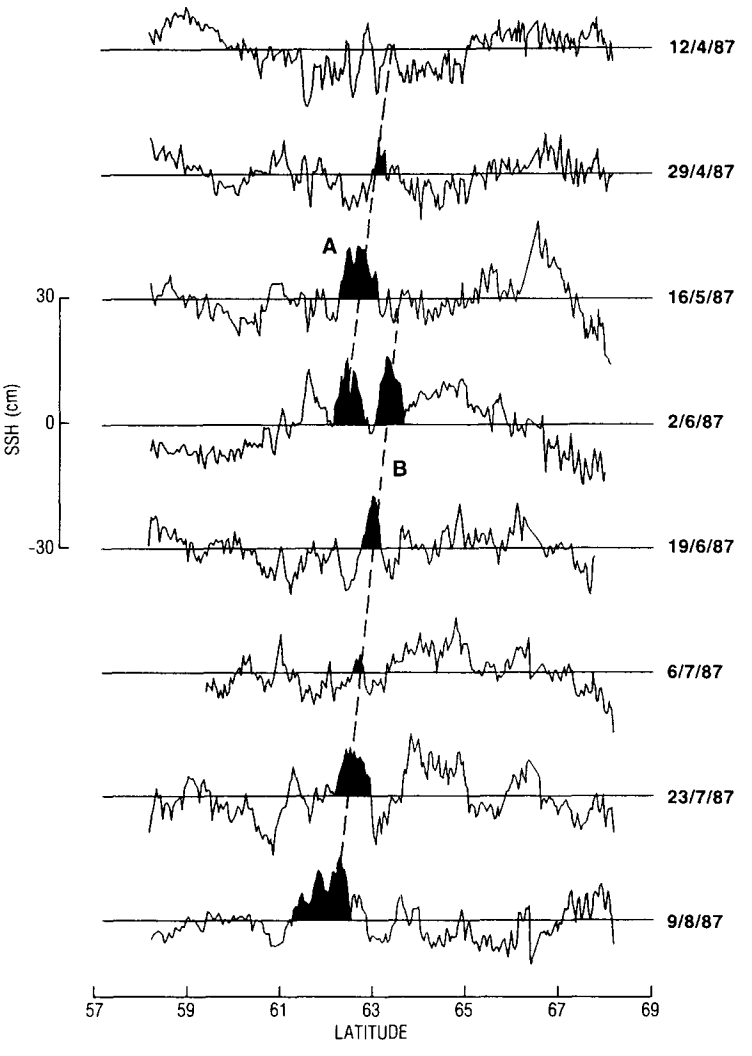

Fig 14 Sequence of SSH profiles at 17 day intervals along ascending track A12 in 1987 (Figs 12 and 13) Meanders in the IFF designated "A" and "B" propagate toward lower latitudes (southeast)

propagation speeds in this sequence are similar to the 1987 meanders. Fortunately, one of the drifters (F2) became entrained in this meander toward the end of 1988, providing additional information on characteristics of these interesting features.

During the 2 weeks prior to its entrainment, average daily speed of the drifter was 7 cm s^{-1}, and during the following 2 weeks after it separated and drifted south in the Faeroe–Shetland Channel, the drift speed averaged 15 cm s^{-1}. However, during its 2 week entrainment period (Fig. 16), the average speed was 27 cm s^{-1}, with a daily average maximum of nearly 50 cm s^{-1}. These latter speeds suggest SSH relief of 18–33 cm above the background. From Fig. 15, the altimeter measured a SSH relief of 20–30 cm. Considering the difference in methods, the comparison is very favorable. Since the drifter

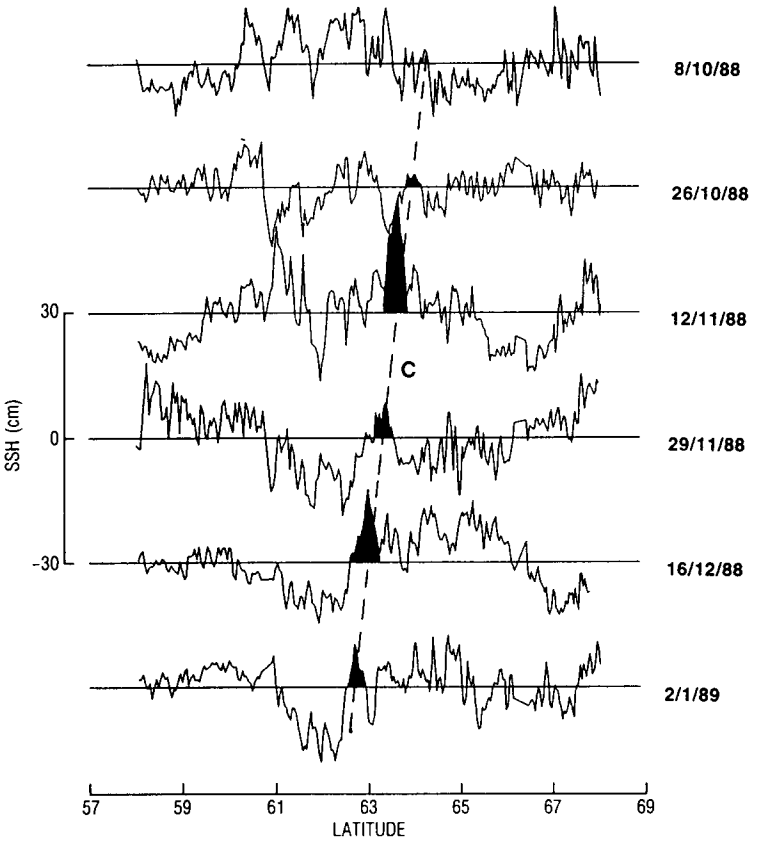

Fig 15 Sequence of SSH profiles at 17 day intervals along ascending track A12 in 1988 Meander "C", shown above, entrained drifter F2 (Fig 16) for about 2 weeks from mid-December through the beginning of 1989

did not continue in a closed anticyclonic turning, it seems reasonable to conclude, as we have done, that these features are meanders of the IFF, and not anticyclonic eddies.

Figure 17 provides an overview of the eastward propagation of the three meanders noted in Figs 14 and 15, as determined along the altimeter track, A12. Even though the altimeter track may not locate the meanders precisely, since it will not necessarily pass through the center of the meander, some reasonable conclusion can be made. First, the meanders are initially detected north of the Faeroe Islands (Figs 14 and 15), at about 6–8°W, 63–64°N, and propagate southeastward, parallel to the north face of the Iceland–Faeroe Ridge. Second, they propagate with similar, and fairly consistent, speeds (about 3.3 km day^{-1}) until they reach the Faeroe–Sheland Channel, where they become lost from view In the western part of the Ridge, the IFF bends southwestward, and departs from the A12 track. For this reason the meander starting point is not clearly discerned. However, examination of the adjacent ascending track (not shown) did not provide any additional evidence for generation of the meanders west of 8°W.

The relatively strong signatures, and lifetimes of 2–3 months, would indicate that these meanders are important to the dynamics of the IFF. Our first inclination suggests that they

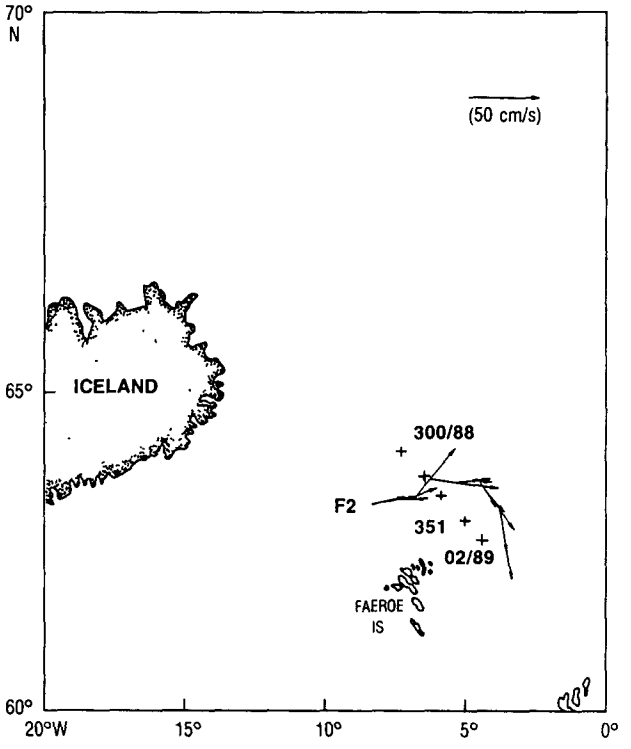

Fig 16 Locations of meander "C" at 17 day intervals (Fig 15) given by plus symbols, dates are Julian Drift vectors from drifter F2 are from daily samples covering the period JD 350 to JD 363, 1988

are associated with the topographic "beta" effect, since propagation is in the proper direction for control by the northern slope of the Ridge. However, simple calculations using the slope of the bottom topography indicate that a topographic "beta" wave would propagate at speeds about one order of magnitude greater than measured speeds. Clearly, there is a need to measure the vertical density and velocity structure of these meanders, concomitant with satellite mapping, in order to properly resolve this interesting issue without resort to speculation.

4 CONCLUSIONS

In this study, GEOSAT altimetry, AVHRR imagery and satellite tracked drifters were used to investigate the Iceland–Faeroe frontal zone. Based upon this experience, the following conclusions can be made:

(a) SSH slope variability from GEOSAT altimetry verified that relatively strong eddy and meander fields occurred on and south of the IFF. In contrast, a relatively quiet field north of the IFF suggested that the front is effective in limiting northward propagation of energy from the North Atlantic side

(b) Along the western side of the IFF (East Iceland shelf), and along the eastern side

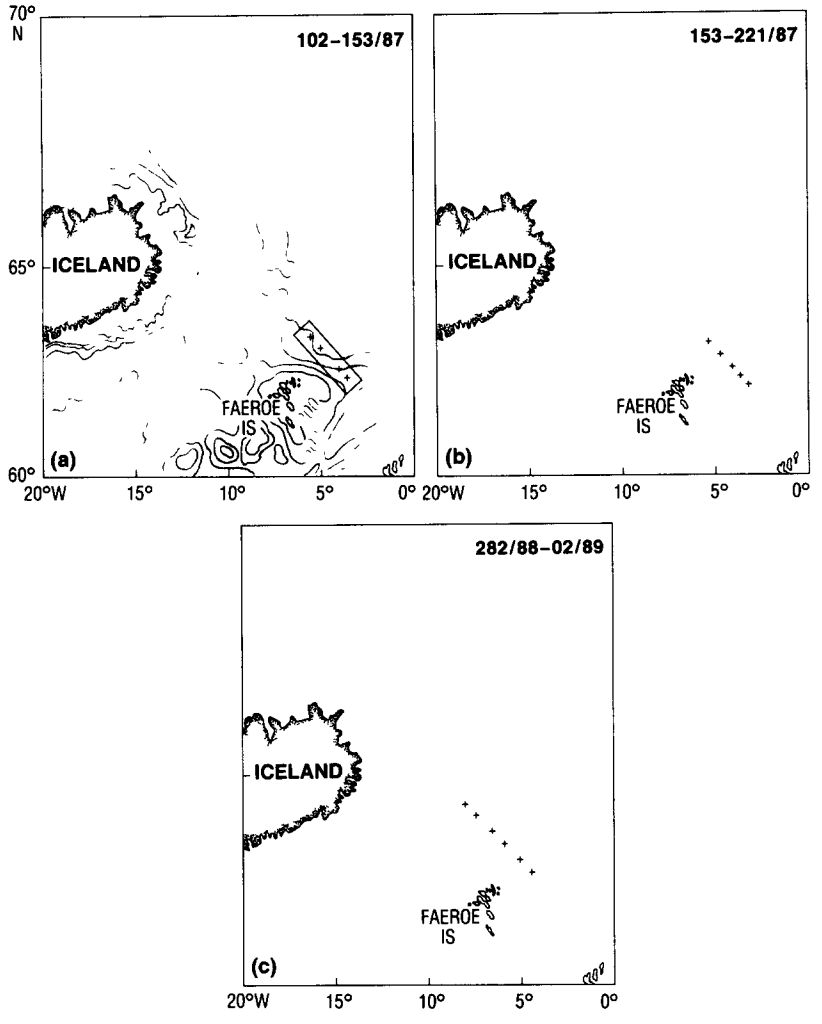

Fig 17 (a) Tracks of meander "A" along ascending track A12 at 17 day intervals, (b) same for meander "B", (c) same for meander "C" Julian dates are located in the upper right corner of each figure

(north of the Faeroe Island), SSH relief (change in SSH over 50 km) was characteristically above 20 cm. However, in the central region of the IFF, SSH relief was characteristically 10–15 cm.

(c) We were unable to unambiguously monitor the location of the IFF using GEOSAT altimetry alone. (1) Although features associated with the IFF could be tracked, the *ca* 10–15 cm topographic relief through the central area of the IFF was insufficient to bring the IFF above background uncertainty (2) Numerous entire-track altimeter data dropouts, especially in the descending tracks, limited the ability to locate the front through repeatable feature identification. We expect considerable improvement in repeatability with future altimeters using better methods of nadir pointing.

(d) Several relatively large (20–30 cm relief) and vigorous (up to 50 cm s^{-1} swirl speed) anticyclonic meanders in the IFF could be tracked via altimetry, and verified by AVHRR and drifters. These meanders, with a *ca* 25 km radius of curvature, were observed north of the Faeroe Islands, propagating eastward at about 3 3 km day^{-1}. Three such meanders were tracked during the 2-year study, with visible lifetimes of 2–3 months duration. Although the location of the meanders on the northern slope of the Ridge and the propagation direction suggested that they might be topographic "beta" waves, propagation speeds were about one order of magnitude less than rough calculations provide for such waves. There is a clear need for measurements of the vertical structure of these meanders concomitant with satellite mapping.

(e) Satellite-tracked drifters were an effective means of verifying feature locations as well as feature amplitudes.

(f) The importance of reliable tidal models in application to altimetry near coastal boundaries and in shallow areas with rough topography must be stressed. Although the Schwiderski model has served well in the deep ocean, we found a significant tidal "kink" over the Ridge which provided a false signal that could readily be confused with the IFF. This confirms the work and conclusions of THOMAS and WOODWORTH (1990) and CARTWRIGHT and RAY (1990).

Although frontal meanders have been the subject of previous papers, this is the first investigation, to our knowledge, in which propagating meander features on the IFF have been clearly identified and the propagation rates measured. The origin, internal structure and dynamics of these interesting features are open questions for future observational and modelling efforts.

Acknowledgements—We are grateful to J Goudeau and R Broome for their help in constructing the drifters, and to T Hopkins for deployment of three of the drifters aboard the SACLANT vessel, *Alliance* C Johnson helped in processing the altimeter data, and F Abel processed the AVHRR images This work was funded by the Office of Naval Research under the GIN Sea Program (Program element 61153N) and the GEOSAT Ocean Applications Program (Program element 63704N) Permission to use the World Ocean Floor map in Fig 1 was kindly granted by Marie Tharp

REFERENCES

BORN G H , J L MITCHELL and G A HEYLER (1987) Geosat—ERM Mission design *Journal of Astronautical Science*, **35**, 119–134

BOYD J D (1988) Aircraft measurements in the Norwegian and Iceland Seas during "Chair Helix," October 1987 NORDA Tech Note 400, September, 1988

BODY J D , P W MAY and J W MCCAFFREY (1987) Preliminary report environmental conditions in the Norwegian–Iceland Seas, May 1987 NORDA Tech Note 341, June, 1987

CARTWRIGHT D E and R D RAY (1990) Oceanic tides from GEOSAT altimetry *Journal of Geophysical Research*, **95**, 3069–3090

CHENEY R E and J G MARSH (1981) SEASAT altimeter observations of dynamic topography in the Gulf Stream region *Journal of Geophysical Research*, **86**, 473–483

DOBSON E B (1988) Dynamic topography as measured by the GEOSAT altimeter in regions of small surface height signatures Proceedings of IGARSS '88 Symposium, Edinburgh, Scotland, 13–16 September 1988 Ref ESA SP-284 (IEEE 88CH2497-6) Published by ESA Publication Division, August 1988.

DOREY S W (1978) Current-meter Data Report for observations between Iceland and Norway during 1975 and 1976, NAVOCEANO TN-3431-01-78 Washington D C , US Naval Oceanographic Office

FLATHER R A (1981) Results from a model of the north east Atlantic relating to the Norwegian Coastal Current In: *The Norwegian Coastal Current*, Vol 2, R SAETRE and M MORK, editors, University of Bergen, Bergen, Norway, pp 427–458

GOTTHARD G A (1974) Observed variations of the UK–Iceland GAP front, NAVOCEANO TN-6150-20-74 Washington D C , US Naval Oceanographic Office

HANSER B and J MEINCKE (1979) Eddies and meanders in the Iceland–Faroe ridge area *Deep-Sea Research*, **26**, 1067–1082

HELLAND-HANSEN B and F NANSEN (1909) The Norwegian Sea *Report on Norwegian Fishery and Marine Investigations*, **2**, 1–359

HOPKINS T S (1988) The GINSEA, Review of Physical Oceanography and Literature from 1972 Saclancen Report, Serial No SR-124 La Spezia, Italy, Saclant Undersea Research Centre

JOHANNESSEN J A (1984) Can eddies in the Norwegian–Greenland and Barents Seas be detected with radar altimeter? Proceedings of workshop on ERS-1 radar altimeter data products, Frascati, Italy, 8–11 May, 1984, ESA SP-221, August 1984

JOHANNESSEN O M (1986) Brief overview of the physical oceanography In *The Nordic Seas*, B G HURDLE, editor, Springer-Verlag, New York, pp 103–127

LYBANON M and R L CROUT (1987) The NORDA GEOSAT Ocean Applications Program *Johns Hopkins APL Technical Digest*, **8**, 212–218

LYBANON M , R L CROUT, C H JOHNSON and P PISTEK (1990) Operational altimeter-derived oceanographic information the NORDA GEOSAT Ocean Applications Program *Journal of Atmospheric and Oceanic Technology*, **7**, 357–376

MCARTHUR J L , P C MARTH JR and J G WALL (1987) The GEOSAT radar altimeter *Johns Hopkins APL Digest*, **8**, 176–181

MITCHELL J L , J M DASTUGUE, W J TEAGUE and Z R HALLOCK (1990) The estimation of geoid profiles in the NW Atlantic from simultaneous satellite altimetry and AXBT sections *Journal of Geophysical Research*, **95**, 17965–17977

PISTEK P , P J MINNETT, S A PIACSEK and J SELLSCHOPP (submitted) GEOSAT altimeter measurements of sea-surface height over the Norwegian Sea *Journal of Geophysical Research*

PORTER D L (1988) Determination of Gulf Stream positions utilizing GEOSAT altimetry data and a 22 cycle mean sea surface Johns Hopkins/APL Technical Report No S1R88U-024

ROBINSON A R , L J WALSTAD, J CALMAN, E B DOBSON, D W DENBO, S M GLENN, D L PORTER and J GOLDHIRSH (1989) Frontal signals east of Iceland from the GEOSAT altimeter *Geophysical Research Letters*, **16**, 77–80

SCHWIDERSKI E W (1980) On charting global ocean tides *Review of Geophysics and Space Physics*, **18**, 243–268

SCOTT J C and A L MCDOWALL (1990) Cross-frontal cold jets near Iceland in-water, satellite infrared, and GEOSAT altimeter data *Journal of Geophysical Research*, **95**, 18005–18014

SMART J H (1984) Spatial variability of major frontal systems in the North Atlantic–Norwegian Sea area 1980–81 *Journal of Physical Oceanography*, **14**, 185–192

TAI C -K (1989) Accuracy assessment of widely used orbit error approximations in satellite altimetry *Journal of Atmospheric and Ocean Technology*, **6**, 147–150

THOMAS J P and P L WOODWORTH (1990) The influence of ocean tide model corrections on GEOSAT mesoscale variability maps of the North East Atlantic *Geophysical Research Letters*, **17**, 2389–2392

TRANGELED S (1973) Oceanography of the Norwegian and Greenland Seas and adjacent areas Vol I Bibliography SACLANTCEN SM-4, La Spezia, Italy, Saclant ASW Research Centre

TRANGELED S (1974) Oceanography of the Norwegian and Greenland Seas and adjacent areas Vol II survey of 1870–1970 literature Saclantcen SM-4, La Spezia, Italy, Saclant ASW Research Centre

WILLEBRAND J and J MEINCKE (1980) Statistical analysis of fluctuations in the Iceland–Scotland frontal zone *Deep-Sea Research*, **27**, 1047–1066